Journal of Inorganic Biochemistry 235 (2022) 111935

Contents lists available at ScienceDirect

Journal of Inorganic Biochemistry

journal homepage: www.elsevier.com/locate/jinorgbio

Cobalt(III)- and rhodium(III)-porphyrin complexes for the effective degradation of fentanyl: Biological inactivation and mechanistic insights

Hemant Pal [a], Anneli Nina [a], Okhil K. Nag [b], Christopher D. Chouinard [a], Amanda Pitt [a], Gregory A. Ellis [b], Scott A. Walper [b], Jeffrey Deschamps [b], Aurora Burkus-Matesevac [a], Kathy Maiello [a], James B. Delehanty [b,*], D. Andrew Knight [a,*]

[a] Department of Biomolecular and Chemical Engineering and Sciences, Florida Institute of Technology, 150 West University Boulevard, Melbourne, FL 32922, USA
[b] Center for Bio/Molecular Science and Engineering, US Naval Research Laboratory, 4555 Overlook Avenue, SW, Washington, DC 20375, USA

A B S T R A C T

Cobalt(III) and rhodium(III) complexes containing the water-soluble porphyrin ligand *meso*-tri(4-sulfonatophenyl)mono(4-carboxyphenyl)porphine (C_1S_3TPP), [Rh(C_1S_3TPP)]Na_x•nH_2O (**1**) and [Co(C_1S_3TPP)]Na_x•nH_2O (**2**) were prepared from the direct reaction of free porphyrin and metal chloride salts in refluxing MeOH/DMF or EtOH/H_2O. Compounds **1** and **2** were characterized using UV–vis and ^{1}H NMR spectroscopies, and high-resolution mass spectrometry. Cell culture based assays of opioid receptor activation showed that while the rhodium complex reduced fentanyl opioid activity 113-fold to an IC50 value of 1.7 μM, the cobalt complex reduced fentanyl activity by 160-fold to an IC50 value of 2.4 μM. An oxidative mechanism for fentanyl breakdown is proposed.

1. Introduction

Opioids are a class of drug with a number of medical uses including pain control and anesthesia, however the misuse of these opioids is increasing rapidly. According to the National Institute on Drug Abuse (NIDA), of the 91,799 drug-involved overdose deaths in 2020, 68,630 (75%) were related to opioids (including natural, semi-synthetic, and synthetic versions of the drug class). [1] In comparison to morphine, fentanyl and fentanyl analogs have enhanced activity and potency (50–100×) with fewer adverse effects [2] but the superior potency of novel fentanyl analogs raises particular concerns. [3] The synthesis of novel analogs of increasing potency poses a significant risk not only to individuals, but also to large civilian populations and warfighters through accidental or deliberate exposure, classifying fentanyl as a pharmaceutical based agent (PBA). [4,5] An example of opioid PBAs being used to incapacitate a large population has already been reported. On October 23, 2002, the Russian Special Forces exposed Chechen terrorists to an aerosol containing opioids resulting in 125 deaths *via* respiratory depression and cyanosis. [6] Analysis of clothing and urine samples from the casualties revealed the presence of carfentanil and remifentanil. With potencies of 50-100× and 10,000× greater than morphine, respectively, fentanyl and carfentanil have become the central focus in chemical decontamination and neutralization studies. [3]

In use since 1971, the opioid naloxone (NARCAN®) is currently the state-of-the-art treatment for opioid exposure and overdose. Naloxone is a competitive opioid receptor antagonist and its function is two-fold: (i) it competes with the opioid at the μ-opioid receptor and (ii) it displaces receptor-bound opioid. In this regard, naloxone decreases the activation of the intracellular opioid receptor signaling pathway while allowing the body to naturally clear the opioid through Phase I (oxidation) detoxification pathways *via* iron-containing cytochrome P450 enzymes in the liver. [7] As naloxone merely competes with and displaces bound opioid from the receptor, the administration of multiple doses of the drug are often required until the opioid clearance is achieved and in some cases, the effect of the opioid overdose cannot be overcome, even after repeated dosing. Further, because naloxone interacts directly with the opioid receptor, cessation of administration can induce withdrawal symptoms in response to naturally occurring opioids. In addition, the expression of new opioid receptors as a result of habitual opioid usage can render patients refractory to naloxone treatment due to the over-expression of opioid receptors.

The structures of the majority of naturally occurring and synthetic opioids such as fentanyl, carfentanil and morphine possess a trialkyl amine (-NR_3) group, in addition to various additional functionalities including phenyl, amide and alcohol groups (Fig.1). Of note is the high stability of the tertiary amine in opioids towards hydrolysis, oxidation and de-alkylation thus resulting in long-term environmental persistence. Qi *et al.* reported that strong oxidizing agents, such as peroxides and

* Corresponding authors.
E-mail addresses: james.delehanty@nrl.navy.mil (J.B. Delehanty), aknight@fit.edu (D.A. Knight).

https://doi.org/10.1016/j.jinorgbio.2022.111935
Received 1 May 2022; Received in revised form 3 July 2022; Accepted 13 July 2022
Available online 18 July 2022
0162-0134/Published by Elsevier Inc.

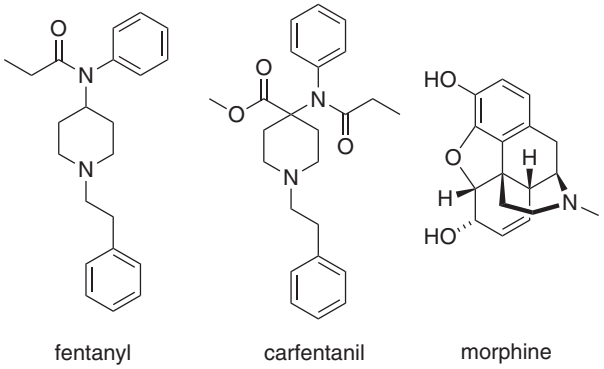

Fig. 1. Structures of common opioids.

hypochlorites, can promote the degradation of fentanyl *via* oxidative *N*-dealkylation at the piperidine ring as the principal pathway, and subsequent formation of norfentanyl which was subsequently broken down further. [8] Additionally, norfentanyl is an inactive fentanyl analogue, [9] therefore making *N*-dealkylation a desirable pathway. Fentanyl also undergoes degradation in the presence of either strong mineral acids (HCl) or strong oxidizers, and both the thermal and photochemical breakdown of the opioid have been investigated. [10,11]

Previously, the aqueous catalytic oxidative *N*-dealkylation of acyclic trialkyl amines using a rhodium porphyin complex was reported. [12] Although fentanyl posseses a cyclic piperidine ring structure, we suggest that metal porphyrin complexes will effectively neutralize fentanyl and analogues *via* an oxidative ring opening mechanism. Herein we describe the synthesis of two metalloporphyrin complexes, RhC_1S_3TPP (**1**) and CoC_1S_3TPP (**2**), for the neutralization of fentanyl in water under mild conditions, and demonstrate complete removal of fentanyl (10 μM) after 6 h using CoC_1S_3TPP. We also propose a possible mechanism for fentanyl degradation involving an unexpected tandem *N*-dealkylation/oxidation reaction. Finally, we show that the metal-porphyrin complexes reduce fentanyl activation of the mμ opioid receptor in living cells by ~160-fold.

2. Experimental

2.1. General data

All reactions and manipulations were conducted in air except for NMR sample preparation which was performed under N_2. All ^1H NMR spectra were recorded on a Bruker Avance 400 spectrometer in DMSO-d_6 and referenced to internal tetramethylsilane (^1H). Spectra were processed using iNMR v3.4. UV–visible absorption spectra were recorded at 25 °C on an HP 8453 diode array spectrometer in 1 cm quartz cuvettes. High-resolution mass spectra were recorded on an Agilent 6560 IM-QTOF operated in positive mode electrospray ionization (ESI) for fentanyl/breakdown product analyses and in negative mode for characterization of the porphyrins. Chromatographic separations were performed using an Agilent 1290 II UHPLC coupled to the Agilent 6560 IM-QTOF. Samples (1 μL) were injected onto an Agilent Zorbax Extend-C18 column (2.1 × 50 mm, 1.8 μM) maintained at 30 °C (mobile phases A: 0.1% formic acid, B: methanol). The flow rate was maintained at 0.400 mL/min. NMR spectra for **1** and **2**, other relevant mass spectrometer instrument parameters, and LC gradient conditions are provided in Appendix A. Supporting information. Reagents and solvents were obtained as follows and used as received: tri(*p*-sulfonatophenyl)mono(*p*-carboxyphenyl)porphyrin tetrasodium salt, C_1S_3TPP (Frontier Scientific); $RhCl_3{\cdot}xH_2O$ (next Chimica); $CoCl_2{\cdot}6H_2O$ (MP Biomedicals, LLC); fentanyl 1 mg/mL in methanol (Supelco); morphine 1 mg/mL in methanol (Supelco); carfentanil (Caymen Chemicals), trifluoroacetic acid (Fisher Scientific); NaOH pellets (Fisher Chemicals); anhydrous methanol (Drisolv); DMF anhydrous (Acros Organics); ethanol (Acros Organics, 99.5+%); DMSO-d_6 + 0.03% TMS, 99.8% atom D (Acros Organics); ethyl acetate (VWR); acetone (VWR); diethyl ether (VWR), aluminum oxide (neutral) Brockmann I (Acros Organics); aluminum oxide (basic) Brockmann I (Sigma Aldrich); Sephadex G-10 (GE Healthcare); Dulbecco's phosphate-buffered saline (1×) (+)calcium chloride (+)magnesium chloride (Gibco); and PBS buffer (MP Biomedicals, LLC or ATCC). For LC-MS the solvents used were methanol, water (0.1% formic acid), and acetonitrile (Fisher Scientific Optima LC-MS grade). All stock solutions and buffers were freshly prepared, and solvent runs for the gravity columns were performed using Millipore Direct-Q 18.2 MΩ H_2O and/or LCMS grade H_2O. Microanalyses were not determined for complexes **1** and **2** due to variable degrees of hydration or sodiation. G418 sulfate solution (1 mg/mL), antibiotic-antimycotic, 3-isobutyl-1-methylxanthine (IBMX), 4-(3-butoxy-4-methoxybenzyl) imidazolidone (Ro 20–1724, and forskolin were obtained from Millipore Sigma. 4-(2-hydroxyethyl)-1-piperazineethanesulfonic acid (HEPES, 1 M), Dulbecco's Modified Eagle Medium (DMEM) containing 25 mM HEPES (DMEM-HEPES), live cell imaging solution (LCIS) were purchased from ThermoFisher. Fetal bovine serum (FBS) and Kaighn's modification of Ham's F12 medium (F-12 K) were purchased from ATCC. Chinese hamster ovary cells (CHO-K1 cells, cat# ES-542-C) stably with transfected with human μ Opioid Receptor (OP_3) was obtained from PerkinElmer.

2.2. Synthesis of $Na_2[(C_1S_3TPP)Rh]$ (1)

A 50 mL round-bottom flask was charged with rhodium trichloride hydrate, 38–40% Rh (0.1002 g, 0.3805 mmol), anhydrous DMF (10 mL) and refluxed until the solution became yellow (ca. 30 min). The solution was transferred to a 500 mL round-bottom flask containing a solution of C_1S_3TPP (0.0574 g, 0.0581 mmol) in CH_3OH (150 mL), and refluxed for 30 min. After allowing the solution to cool to room temperature, DI H_2O (50 mL) was added, the solution was reduced to 10 mL using rotary evaporation and chromatographed on a 31 mm diameter column (Al_2O_3, 0.02 M NaOH) to remove unwanted rhodium salts. The solution was then chromatographed on a Sephadex G-10 column using H_2O as the eluent and further purified using dialysis (Spectra/Por® dialysis membrane, MWCO = 0.5–1.0 kD). During dialysis, the external water was replaced periodically every 8 h until a constant pH was obtained. The solution was freeze-dried to give **1** as a purple solid. Crude yield was 0.0216 g. UV–Vis (H_2O): [λ_{max}, nm (ε, M^{-1} cm^{-1})]: 419 (149,191), 529 (31,646), 560 (17,533) ^1H NMR (400 MHz, DMSO-d_6): δ (ppm): 9.03–8.88 (m, 8H), 8.37 (s, br., 2H), 8.26–8.23 (m, 8H), 8.10–8.07 (m, 6H). LC-IM-MS: m/z $[M + H]^+$ = 497.9845, calcd. 497.9874.

2.3. Synthesis of $Na_2[(C_1S_3TPP)co]$ (2)

A 500 mL round bottom flask was charged with cobalt dichloride hexahydrate (0.0122 g, 0.0513 mmol), C_1S_3TPP (0.0499 g, 0.0506 mmol), H_2O (15 mL), and ethanol (150 mL), and refluxed for 45 min. The solvent was removed using rotary evaporation. H_2O (10 mL) was added to the residue which was chromatographed on a 31 mm diameter column (Al_2O_3, 71.0 g, H_2O-MeOH-acetone, 7/2/1, v/v). The solution was then chromatographed on a Sephadex G-10 column using H_2O as the eluent. The eluate was reduced using rotary evaporation and cold acetone (50 mL) was added to precipitate a solid which was collected *via* centrifugation, washed with acetone (3 × 10 mL), diethyl ether (3 × 2 mL) and then dried under vacuum to give **2** as an orange-red solid. Crude yield: 0.0384 g. UV–Vis (H_2O): [λ_{max}, nm (ε, M^{-1} cm^{-1})]: 425 (62,275), 541 (8165) ^1H NMR (400 MH_Z, DMSO-d_6): δ (ppm): 8.75 (s, 8H), 8.25 (d, J = 8.08 Hz, 2H), 8.05–7.97 (m, 14H), LC-IM-MS: m/z $[M + H]^+$ = 317.3344, calcd. 317.9984.

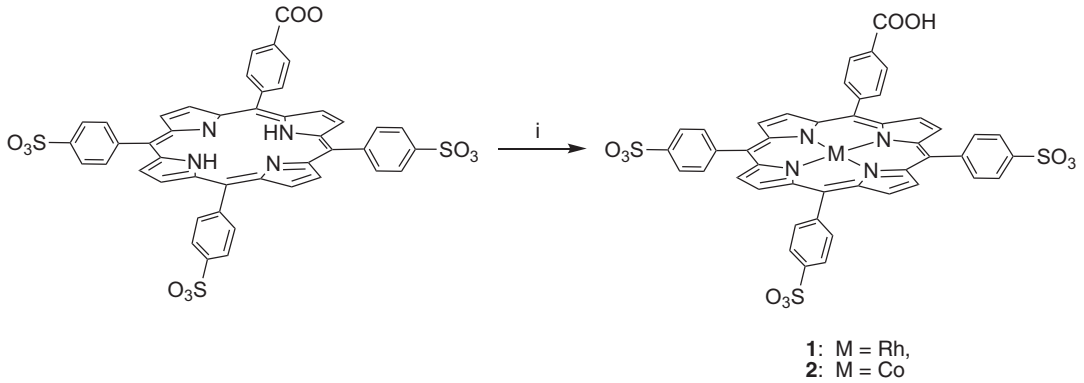

Fig. 2. Synthesis of metal porphyrin complexes **1** and **2**. (i) **1**: $RhCl_3 \bullet xH_2O$, DMF, reflux, 2 h; **2**: $CoCl_2 \bullet H_2O$, $EtOH/H_2O$, reflux, 45 min. Counterions and waters of hydration not shown.

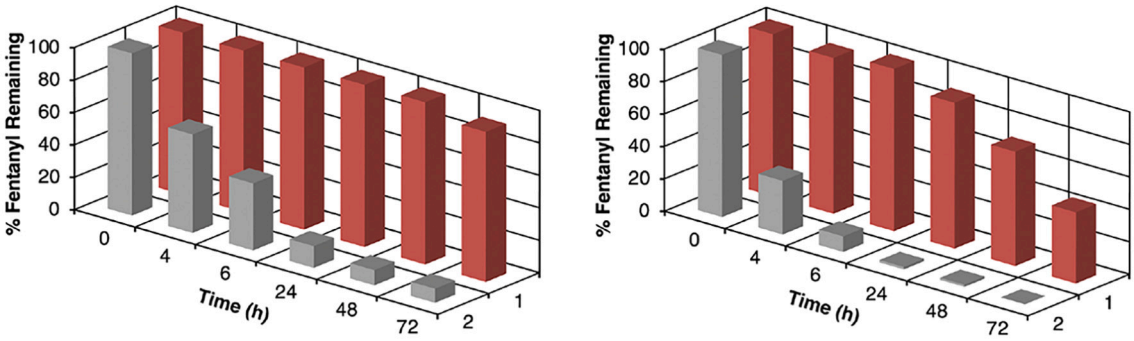

Fig. 3. Disappearance of fentanyl throughout reaction with rhodium (**1**) and cobalt (**2**) porphyrin complexes. (A) [Complex]:[Fentanyl] = 1:1. (B) [Complex]:[Fentanyl] = 5:1 (Conditions: 37 °C, [Fentanyl] = 10 μM).

2.4. Opioid removal and degradation studies

Amber screw-capped vials (4 mL) were charged with DI water, opioid, metal complex and a micro-stirrer bar. Initial concentrations of stock solutions of complex **1** and **2** were 1.86×10^{-4} M and 6.00×10^{-4} M, respectively. The reactions were stirred continuously (800 rpm) at 37 °C using a programmable hot-plate stirrer equipped with an anodized aluminum heat block. Aliquots (200 μL) were removed at time points using a micro-pipettor, transferred to LC vials, frozen with liquid nitrogen, stored at −10 °C and then analyzed after 12 h using LC-MS. The disappearance of opioids over time was determined by measuring changes in the chromatographic peak area of extracted ion chromatograms (EICs) for protonated fentanyl, $[M + H]^+$ at *m/z* 337.228. Additional peaks appearing in the chromatographic separations (compared with control samples) were analyzed, and putative chemical formulae for breakdown products determined based on exact mass using Agilent MassHunter Qualitative Analysis 10.0 software. Additionally, untargeted MS/MS data was acquired using data-dependent acquisition (DDA); fragmentation spectra were further used to determine chemical formulae and structure.

2.5. Cell culture and opioid receptor activation assay

CHO-K1 stably expressing the mμ opioid receptor cells were cultured according to the manufacturer's protocol. Briefly, the cells were cultured in F-12 K growth medium supplemented with 10% FBS, 1% antibiotic-antimycotic, and 0.4 mg/mL G418 in a standard humidified atmosphere containing 5% CO_2 at 37 °C. The culture media was changed every other day, and at ~80% confluency, the cells were trypsinized (0.05% trypsin / 0.5 mM EDTA) and subcultured. Opioid receptor activation was performed using the cAMP-Glo™ Assay kit (Promega, Madison, WI) according to the manufacturer protocol. This chemiluminescent assay measures the cellular pool of ATP as an indicator of opioid-mediated inhibition of cAMP formation. For the cAMP assay, the cells were plated in a clear-bottom 96 well plate (~20 k cells/well) cultured for 24 h. Briefly, the cells were washed with DMEM followed by 45 min incubation with fentanyl or fentanyl/**1** or fentanyl/**2** at different concentrations (0–250 μM) in phosphodiesterase inhibitor induction buffer (500 μM IBMX and 100 μM Ro 20–1724 in DMEM) at 37 °C. Then, the antagonist solutions were removed, and forskolin (5 μM, in induction buffer) was added to each well followed by another incubation for 15 min at 37 °C. The forskolin solution was removed by aspiration, and the cells in the wells were lysed using the lysis buffer supplied with cAMP-Glo™ Assay kit. Detection and quantification of the luminescence response was read on a Tecan Spark Cyto 600 (Tecan U.S.)

3. Results and discussion

3.1. Synthesis and characterization of porphyrin complexes

The synthesis of C_1S_3TPP complexes of rhodium and cobalt was achieved *via* a direct metallation reaction of metal salt with free base in refluxing solvent as shown in Fig. 2. The presence of the benzoic acid group will allow us to further modify the complexes (e.g., conjugation to amine-functionalized nanoparticles and other nano-drug delivery systems) in future studies. After isolation using a combination of column chromatography, ion-exchange chromatography or dialysis, the rhodium and cobalt complexes **1** and **2** were obtained as purple and red solids respectively. The complexes are stable for long periods of time in aqueous solution and air. Although elemental analysis was performed, varying degrees of hydration as demonstrated by ^1H NMR and thermogravimetric analysis (TGA) for different batches precluded

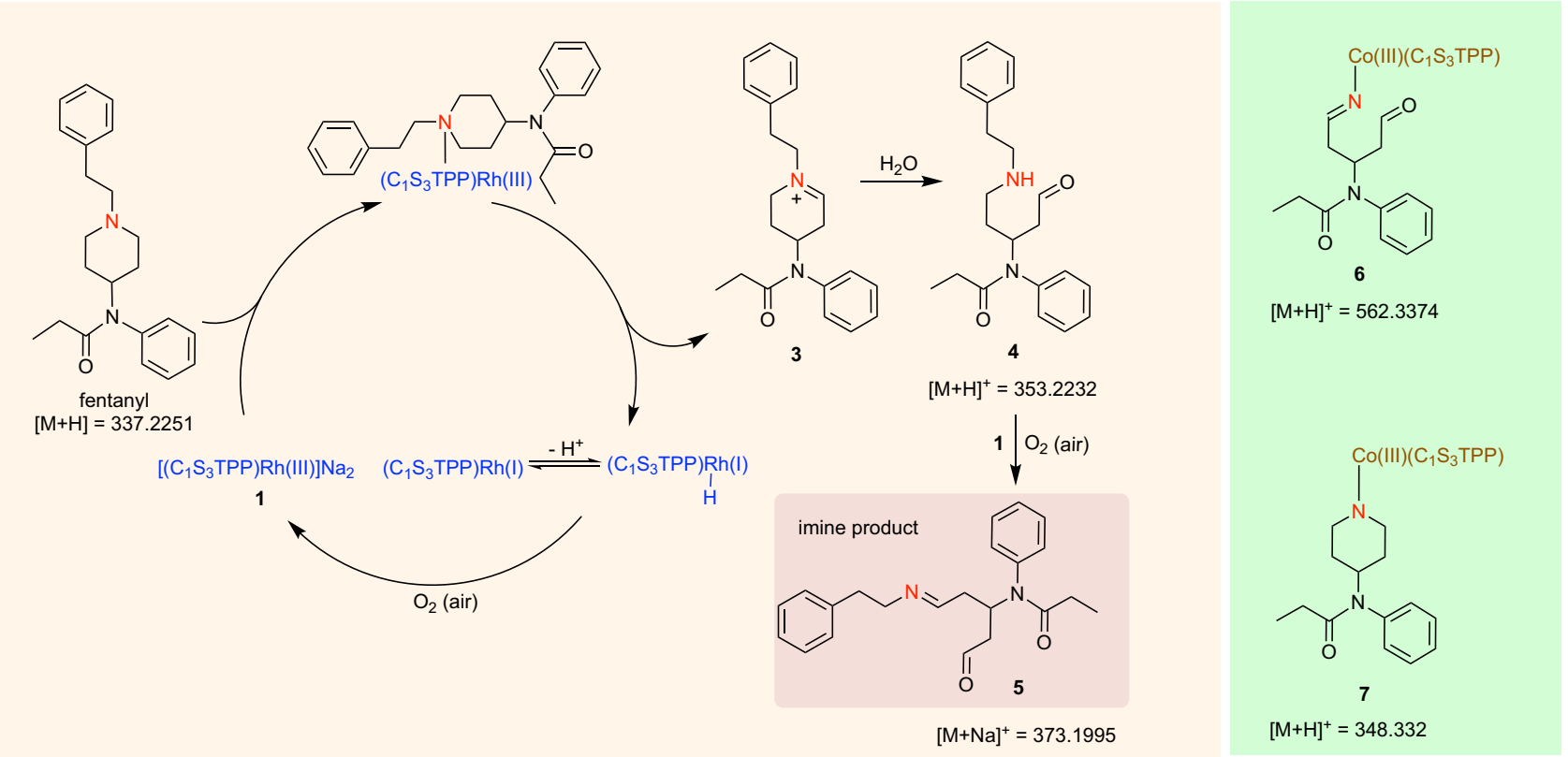

Fig. 4. Proposed mechanism for the rhodium-porphyrin mediated tandem dealkylation-oxidation of fentanyl (left). Adducts formed from cobalt pophyrin mediated dealkylation of fentanyl.

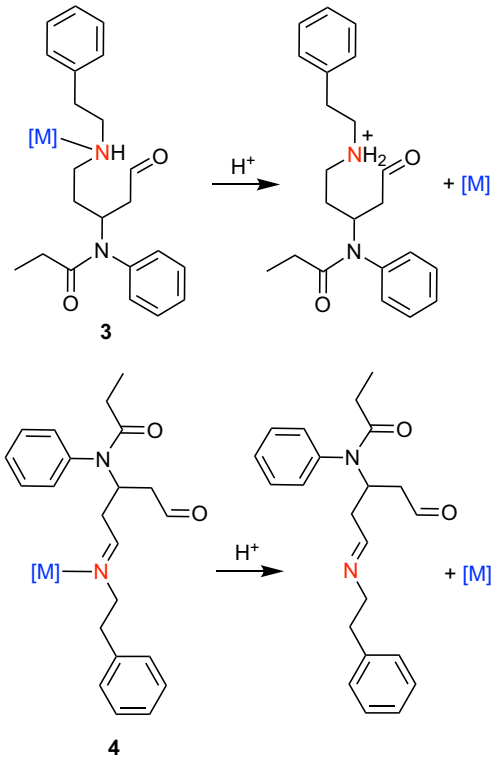

Fig. 5. Protonation of metal-coordinated secondary amine and imine intermediates in TFA promoted fentanyl degradation.

assignment of an exact number of waters of hydration to the molecular formulas. All attempts at crystallization of both **1** and **2** using a variety of methods (vapor diffusion, slow cooling of warm, saturated solution, solvent layering) were unsuccessful and variation in the waters of hydration, however poor success in recrystallization is not unusual for water-soluble metalloporphyrins, especially those with low symmetry. [13] Analytical purity of the metal-porphyrin was confirmed using HR-MS (*vide infra*).

Characterization of complexes **1** and **2** was achieved using UV–vis and ^{1}H NMR spectroscopy and high-resolution mass-spectrometry (HR-MS). The electronic absorption spectra of metalloporphyrins recorded in water, contained a strong transition at 419 nm (**1**) and 425 nm (**2**) and this corresponds to the Soret (or B band) involving a transition to the second excited state ($S_o \rightarrow S_2$). A second weaker transition or multiple transitions corresponding to the first excited state ($S_o \rightarrow S_1$) (Q band(s)) was observed at 529 and 560 nm (**1**), and 541 nm (**2**). The wavelength and extinction coefficient values for the Soret band are in typical ranges for metalloporphyrins [14] and similar to those for Rh(TPPS)$(H_2O)_2$ and Co(TPPS). [15] At relatively high concentrations of **1** (>10 μM), considerable spectral line broadening and decrease in relative intensity was observed, which is likely due to the formation of porphryrin dimers and higher aggregates. [16]

Proton (1H) NMR studies were performed on complexes **1** and **2** in DMSO-d_6 and show no unexpected features. Pyrrole protons resonate as singlets at 8.35 (**1**) and 8.25 (**2**) ppm and the remaining aromatic phenyl protons are seen as multiplets in the regions 9.03–8.07 (**2**) and 8.75–7.97 (**2**) ppm.

3.2. Removal and degradation of fentanyl

To determine the efficacy of rhodium- and cobalt-porphyrin mediated degradation of fentanyl in aqueous solution, reactions between **1** or **2** and 10 μM solutions of fentanyl at various ratios of complex to fentanyl were incubated with stirring at 37 °C in glass vials. At periodic intervals, 200 μL aliquots of the reaction mixture were removed and analyzed using LC-MS. Control reactions in which the metal complex or fentanyl were absent were included in the analysis. The relative amount of fentanyl present was determined from extracted ion chromatograms and any additional peaks due to fentanyl breakdown were identified by HR-MS. Fig. 3 presents a comparison of the activity of complex **1** vs complex **2** for complex:substrate ratios of 1:1 and 5:1 over a period of 72 h. Clearly, cobalt complex **2** is more effective in removing fentanyl with 66.9% removal after 4 h, 90.4% removal after 6 h and complete removal after a 24 h period. Mass spectral analysis and identification of the organic breakdown products from the reaction of complex **1** with fentanyl reveals the presence of an amino-aldehyde **4** which we suggest originates from piperidine ring opening and subsequent hydrolysis (Fig. 4). A second major product was identified as the imine **5**. Interestingly for the reaction with **2**, only adducts of cobalt-fentanyl breakdown products **6** and **7** were detected. The suggested mechanism for the origin of **4** and **5** is described below. Breakdown products **4** and **5** were not quantified.

3.3. Proposed catalytic cycle and mechanism of fentanyl degradation

The proposed catalytic cycle for the removal of fentanyl by metal porphyrin complexes **1** and **2** is shown in Fig. 4 and can be summarized as a tandem dealkylation-oxidation reaction. Mass spectral analysis of the reaction between fentanyl and rhodium complex **1**, reveals the presence of two distinct fentanyl breakdown products: an amino-aldehyde **4** ($[M + H]^+ = 353.322$) resulting from α-carbon oxidation and concomitant ring opening of cyclic iminium intermediate **3** (not observed), which subsequently undergoes oxidation to the final Schiff base product **5** which is observed in the mass spectrum as a sodium adduct ($[M + Na]^+ = 373.199$). The source of the Na^+ is most likely the counter-ion present in complex **1** although sodium is also known to be ubiquitous in analytical grade solvents. Transition metal complexes are known to catalyze the dealkylation of tertiary amines and ring-opening of cyclic amines. For example, Ling *et al.* reported the use of a rhodium porphyrin complex for the aerobic oxidative *N*-dealkylation of a series of tertiary amines in water [12] and the ring opening of *N*-acyl cyclic amines using an iron oligo-pyridine complex with oxone as an oxidant was described by Liu *et al.* [17]. Although complex **1** is used here in our example for piperdine ring opening and subsequent neutralization of opioid activity, the complex may also have a synthetic application in ring-opening functionalization of unstrained cyclic amines. [18] To complete the catalytic cycle, following elimination of the iminium intermediate **3**, C_1S_3TPPRh(III) is regenerated *via* aerobic oxidation of a rhodium hydride species which subsequently coordinates to fentanyl allowing for turnover. A similar mechanism has been proposed for the oxidation cleavage of acyclic *N*-alkyl amines using (TSPP)Rh(III). [12] Mass spectral analysis of the reaction mixture using the analogous cobalt complex **2** did not show the presence of discreet organic breakdown products but cobalt porphyrin adducts resulting from oxidative dealkylation of fentanyl at $m/z = 562.337$ and simple dealkylation of fentanyl at $m/z = 548.332$. The mechanism for the novel cobalt mediated dealkylation reaction is currently being investigated.

To provide further evidence for the mechanism shown in Fig. 4, the degradation reactions were performed using complex **2** in the presence of (a) trifluoracetic acid (TFA) and (b) pyridine. The addition of TFA is expected to promote protonation of a cobalt coordinated secondary amine (**3**) or imine (**4**) during the catalytic cycle, releasing the free complex as the corresponding hydride and allowing the catalysis to proceed as suggested by Ling *et al.* [12] (Fig. 5).

Fig. 6 shows the difference in the rate of removal of fentanyl in the reaction promoted by **2** with varying ratios of catalyst to substrate and in the presence or absence of TFA. Clearly TFA accelerates the rate of disappearance of fentanyl with complete removal after 6 h and the identity and relative distributions of breakdown products is identical to the reaction without added acid. A control reaction with TFA in the

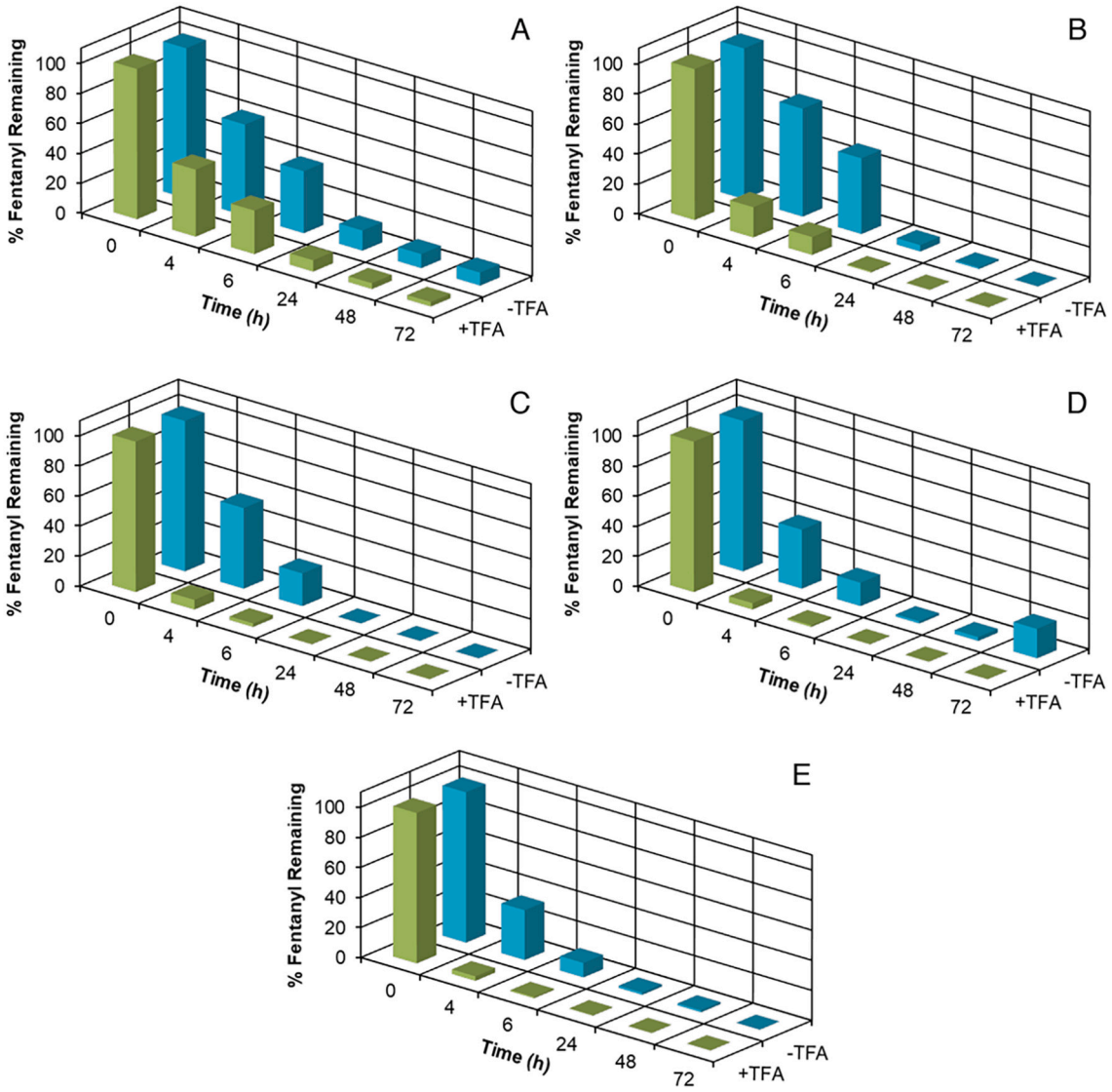

Fig. 6. Change in % fentanyl vs time in the presence of **2**, +/− 0.7 mM trifluoracetic acid in water determined by TOF-MS. (**A**) [Complex]:[Fentanyl] = 1:1. (**B**) [Complex]:[Fentanyl] = 2:1 (**C**) [Complex]:[Fentanyl] = 3:1 (**D**) [Complex]:[Fentanyl] = 4:1 (**E**) [Complex]:[Fentanyl] = 5:1 (Conditions: 37 °C, [Fentanyl]: 10 μM), $[TFA]_{final}$: 8.0 μM).

absence of catalyst showed no change in fentanyl concentration over a 72 h period. For the reaction of fentanyl with complex **1** or **2** performed in the presence of the coordinating ligand pyridine (pyridine:complex = 100:1), complete supression of fentanyl removal and formation of products was observed, consistent with competitive coordination of pyridine vs fentanyl. Finally, as supporting evidence for the oxidative mechanism shown in Fig. 4, reactions of complexes 1 and 2 with fentanyl were performed under argon. In these cases, oxidation products were not observed however new dealkylation products were detected using mass spectrometry. The formation of these products *via* an aerobic mechanism will be the subject of future studies.

3.4. Biological assays

To ascertain the biological activity of fentanyl after its incubation with the Rh- or Co-porphyrin complexes **1** and **2**, we employed a classical cell-based opioid receptor activation assay (Fig. 7). Chinese hamster ovary cells that stably express the mu opioid receptor were incubated with fentanyl alone or fentanyl that was treated with equimolar **1** or **2** for 24 h. The ability of fentanyl to inhibit the formation of cyclic AMP is determined by measuring the increase in cellular levels of free ATP. Here, an increase in chemiluminescence intensity quantitatively tracks active fentanyl in a dose dependent manner. While **1** reduced the opioid activity of fentanyl ~113-fold from an IC50 of 15 nM to 1.7 μM, **2** reduced fentanyl activity ~160-fold to 2.4 μM. This corresponds to a 42% increase in the fentanyl-neutralizing activity for the cobalt complex **2** compared to the rhodium complex **1**.

4. Conclusions

Novel rhodium and cobalt porphyrin complexes exhibit removal of fentanyl from aqueous solution, with the cobalt complex showing the highest activity – complete removal after 24 h and 6 h in the presence of trifluoroacetic acid. Mass spectral analysis indicates a catalytic breakdown of fentanyl *via* a tandem *N*-dealkylation-oxidation pathway for the rhodium complex. Cellular assays demonstrate distinct differences in the fentanyl neutralization activity between the rhodium and cobalt complexes with the cobalt complex exhibiting the ability to neutralize fentanyl activation of the mu opioid receptor ~160-fold compared to fentanyl alone. Finally, preliminary studies indicate that the iron porphyrin complex $C_1S_4TPPFe(III)$ is also active for fentanyl breakdown. A detailed description of this reaction will appear in a future report.

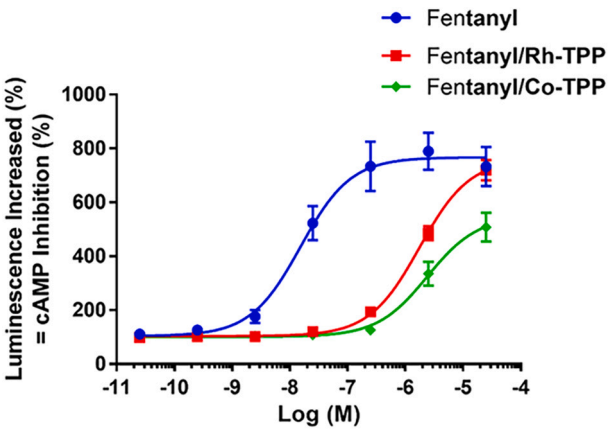

Fig. 7. Opioid activity of fentanyl incubated with **1** (Rh-TPP) and **2** (Co-TPP). Fentanyl (0.5 mM) was incubated at equimolar concentration with **1** or **2** for 24 h at 37 °C. The resulting products were assayed in a mu opioid receptor activation assay. Untreated fentanyl exhibits an IC50 of 15 nM while the IC50 of fentanyl incubated with **1** or **2** was 1.7 μM or 2.4 μM, respectively. Complex **2** shows ~42% greater reduction in the activity of fentanyl compared to Complex **1**.

CRediT authorship contribution statement

Hemant Pal: Investigation, Methodology. **Anneli Nina:** Investigation, Methodology, Writing – original draft. **Okhil K. Nag:** Conceptualization, Writing – review & editing, Investigation, Methodology, Formal analysis. **Christopher D. Chouinard:** Methodology, Formal analysis. **Amanda Pitt:** Methodology. **Gregory A. Ellis:** Investigation. **Scott A. Walper:** Investigation, Methodology. **Jeffrey Deschamps:** Investigation. **Aurora Burkus-Matesevac:** Formal analysis. **Kathy Maiello:** Investigation. **James B. Delehanty:** Funding acquisition, Conceptualization, Writing – review & editing. **D. Andrew Knight:** Conceptualization, Writing – review & editing.

Declaration of Competing Interest

The authors declare that they have no known competing financial interests or personal relationships that could have appeared to influence the work reported in this paper.

Data availability

Data will be made available on request.

Acknowledgments

This work received support from the Defense Threat Reduction Agency-Joint Science and Technology Office for Chemical and Biological Defense (MIPR # N00173-20-2-C009).

Appendix A. Supplementary data

Supplementary data to this article can be found online at https://doi.org/10.1016/j.jinorgbio.2022.111935.

References

[1] Overdose Death Rates. https://nida.nih.gov/drug-topics/trends-statistics/overdose-death-rates, 2022 (Accessed 4 March, 2022).
[2] P.W.H. Peng, A.N. Sandler, A review on the use of fentanyl analgesia in the management of acute pain in adults, Anesthesiology 90 (1999) 576–599.
[3] M. Wilde, S. Pichini, R. Pacifici, A. Tagliabracci, F.P. Busardò, V. Auwärter, R. Solimini, Metabolic pathways and potencies of new fentanyl analogs, Front. Pharmacol. 10 (2019) 1–16.
[4] D.J. Heslop, P.G. Blain, Threat potential of pharmaceutical based agents, Intell. Natl. Secur. 35 (2020) 539–555.
[5] J.P. Caves, Fentanyl as a chemical weapon, CSWMP Proceedings (2019) 1–5.
[6] P.M. Wax, C.E. Becker, S.C. Curry, Unexpected "gas" casualties in Moscow: a medical toxicology perspective, Ann. Emerg. Med. 41 (2003) 700–705.
[7] G.L. Holmquist, Opioid metabolism and effects of cytochrome P450, Pain Med. (Supp. 1) (2009) S20–S29.
[8] L. Qi, Z. Cheng, G. Zuo, S. Li, Q. Fan, Oxidative degradation of fentanyl in aqueous solutions of peroxides and hypochlorites, Def. Sci. J. 61 (2011) 30–35.
[9] O.H. Drummer, Fatalities caused by novel opioids: a review, Forensic Sci. Res. 4 (2019) 95–110.
[10] A. Garg, D.W. Solas, L.H. Takahashi, J.V. Cassella, Forced degradation of fentanyl: identification and analysis of impurities and degradants, J. Pharm. Biomed. 53 (2010) 325–334.
[11] J. Trawiński, P. Szpot, M. Zawadzki, R. Skibiński, Photochemical transformation of fentanyl under the simulated solar radiation – enhancement of the process by heterogeneous photocatalysis and *in silico* analysis of toxicity, Sci. Total Environ. 791 (2021) 148171–148186.
[12] Z. Ling, L. Yun, L. Liu, B. Wu, X. Fu, Aerobic oxidative *N*-dealkylation of tertiary amines in aqueous solution catalyzed by rhodium porphyrins, Chem. Commun. 49 (2013) 4214–4216.
[13] K.R. Ashley, J.G. Leipoldt, V.K. Joshi, Kinetic and equilibrium study of the reaction of (meso-tetrakis(*p*-sulfonatophenyl)porphinato)diaquochromate(III) with thiocyanate ion in aqueous solution, Inorg. Chem. 19 (1980) 1608–1612.
[14] R. Giovannetti, The use of spectrophotometry UV-vis for the study of porphyrins, in: J. Uddin (Ed.), Macro to Nano Spectroscopy, IntechOpen, London, 2012.
[15] S.D. Gokakakar, A.V. Salker, Synthesis, purification and thermal behavior of sulfonated metalloporphyrins, J. Therm. Anal. Calorim. 109 (2012) 1487–1492.
[16] J. Karolczak, D. Kowalska, A. Lukaszewicz, A. Maciejewski, R.P. Steer, Photophysical studies of porphyrins and metalloporphyrins: accurate measurements of fluorescence spectra and fluorescence quantum yields for Soret band excitation of zinc tetraphenylporphyrin, J. Phys. Chem. A. 108 (2004) 4570–4575.
[17] P. Liu, Y. Liu, E.L.-M. Wong, S. Xiang, C.-M. Che, Iron oligopyridine complexes as efficient catalysts for practical oxidation of arenes, alkanes, tertiary amines and *N*-acyl cyclic amines with oxone, Chem. Sci. 2 (2011) 2187–2195.
[18] Y. Kim, J. Heo, D. Kim, S. Chang, S. Seo, Ring-opening functionalizations of unstrained cyclic amines enabled by difluorocarbene transfer, Nat. Commun. 11 (2020) 1–11.